^{125}Te and ^{51}V static NMR study of V_2O_5-TeO_2 glasses

2000 J. Phys.: Condens. Matter 12 2579

(http://iopscience.iop.org/0953-8984/12/12/302)

J. Phys.: Condens. Matter **12** (2000) 2579–2595. Printed in the UK PII: S0953-8984(00)07801-2

^{125}Te and ^{51}V static NMR study of V_2O_5–TeO_2 glasses

Shinichi Sakida†§ Satoshi Hayakawa‡ and Toshinobu Yoko†

† Institute for Chemical Research, Kyoto University, Uji, Kyoto 611-0011, Japan

‡ Faculty of Engineering, Okayama University, Okayama, Okayama 700-0927, Japan

E-mail: sakida@kobe-u.ac.jp

Received 14 September 1999, in final form 7 December 1999

Abstract. The structures of V_2O_5–TeO_2 glasses are investigated by means of ^{125}Te and ^{51}V static NMR spectroscopies and the local structures around the Te and V atoms are discussed in detail from the respective NMR spectra. The fraction of TeO_3 trigonal pyramids increases and that of TeO_4 trigonal bipyramids decreases with increasing V_2O_5 content. The structures of V_2O_5–TeO_2 glasses are quite different from those of tellurite glasses containing network-modifying oxides. The fraction of VO_4 tetrahedra increases and that of VO_5 trigonal bipyramids decreases with increasing V_2O_5 content. Both chains consisting of tellurite structural units and those consisting of vanadate structural units contribute to the formation of the glass network in V_2O_5–TeO_2 glasses.

1. Introduction

V_2O_5–TeO_2 glasses are known as semiconductors [1]. The glasses are highly conductive compared with V_2O_5–P_2O_5 glasses and other glasses containing transition-metal oxides with the same amounts of charge carriers [2–4]. In the V_2O_5–TeO_2 glasses both memory and threshold switching functions have been also reported [5–7].

Although binary tellurite glass systems which can contain less than 50 mol% TeO_2 are few, the binary V_2O_5–TeO_2 system has a very wide glass-forming region. Therefore, the V_2O_5–TeO_2 glasses are of interest from the viewpoint of glass structure. So far, the structures of V_2O_5–TeO_2 glasses have been investigated by means of x-ray diffraction [8] and infrared spectroscopy [9]. As a result, it has been reported that the O coordination environments of Te atoms change from the TeO_4 trigonal bipyramid (tbp) to the TeO_3 trigonal pyramid (tp) with increasing V_2O_5 content. Dimitriev and Dimitrou [8] have concluded that the V atoms are present as VO_5 groups in the examined composition range. Nevertheless, information obtained so far on the structures of V_2O_5–TeO_2 glasses is not sufficient.

NMR spectroscopy is a powerful technique for revealing detailed local structures around nuclei of interest because the direct information about the detailed local structure around the nuclei can be obtained. In previous papers [10–12], the present authors reported that the ^{125}Te static NMR spectra of tellurite glasses can discriminate between TeO_3 tp and TeO_4 tbp and, in addition, estimate the TeO_3 tp and TeO_4 tbp fractions quantitatively. The structures of various vanadate glasses have been investigated by means of ^{51}V NMR spectroscopy and discussed in detail, for example, by Hayakawa *et al* [13, 14]. Thus, since the O coordination environments of the Te and V atoms can be revealed by means of ^{125}Te and ^{51}V NMR spectroscopies, it is

§ Corresponding author. Present address: Venture Business Laboratory, Kobe University, Nada, Kobe 657-8501, Japan.

0953-8984/00/122579+17$30.00

expected to obtain more detailed structures of V_2O_5–TeO_2 glasses by considering the local structures around both Te and V atoms.

In the present work, ^{125}Te and ^{51}V static NMR spectra are measured for V_2O_5–TeO_2 glasses and the structures of V_2O_5–TeO_2 glasses are discussed in detail.

2. Experiment

2.1. Sample preparation

TeO_2 and $xV_2O_5{\cdot}(100-x)TeO_2$ glasses containing no Fe_2O_3 and 0.3 mol% Fe_2O_3 ($x = 5$, 9.1, 20, 30, 33.3, 40, 50, 60 and 70) were prepared. Crystalline $Te_2V_2O_9$ and $NaVTeO_5$ were also prepared for the ^{51}V static NMR measurement. Reagent-grade β-TeO_2 (Mitsuwa Pure Chemicals), Fe_2O_3 (Nacalai Tesque), V_2O_5 (Nacalai Tesque) and Na_2CO_3 (Nacalai Tesque) were used as starting materials. A 3 g batch of well mixed reagents was melted in a 95% Pt–5%Au crucible at 650–800 °C for 10 min in air. The melt was poured onto a stainless plate and immediately pressed by another stainless plate. The TeO_2 glass and the $Te_2V_2O_9$ and $NaVTeO_5$ crystals were prepared according to the procedures described in previous papers [10, 15]. In most cases, the quenched melts were identified to be glassy by visual inspection. In some cases, x-ray diffraction using a Rigaku Geigerflex RAD-IIA diffractometer was used to confirm visual inspection. The melting conditions for all the V_2O_5–TeO_2 glasses are given in table 1.

Table 1. Conditions of glass preparation and V^{4+}/V_{total}.

Glass composition (mol%)	Melting temperature (°C)	Melting time (min)	V^{4+}/V_{total} (%)
$5V_2O_5{\cdot}95TeO_2$	800	10	2.7
$9.1V_2O_5{\cdot}90.9TeO_2$	800	10	3.6
$20V_2O_5{\cdot}80TeO_2$	750	10	5.4
$30V_2O_5{\cdot}70TeO_2$	700	10	6.9
$33.3V_2O_5{\cdot}66.7TeO_2$	650	10	6.6
$40V_2O_5{\cdot}60TeO_2$	700	10	6.4
$50V_2O_5{\cdot}50TeO_2$	700	10	6.4
$60V_2O_5{\cdot}40TeO_2$	750	10	5.1
$70V_2O_5{\cdot}30TeO_2$	750	10	2.4

The experimental uncertainty in the values of V^{4+}/V_{total} is ±0.2%.

2.2. Chemical analysis

The V^{4+}/V_{total} ratios of glass samples were determined by a redox titrimetry using the $KMnO_4$ and $(NH_4)_2Fe(SO_4)_2$ solutions (JIS G1221).

2.3. NMR measurements

The ^{125}Te static NMR spectra of powdered tellurite glasses and crystals were measured at 126.32 MHz (9.4 T) using a JEOL JNM-GSX 400 MAS FT-NMR spectrometer. A single pulse sequence was used for V_2O_5–TeO_2 glasses: a pulse length of 2.5 μs, an accumulation of 12 000–20 000 scans and a pulse delay of 2.5 s. Telluric acid $Te(OH)_6$ was used as a secondary standard, whose chemical shift is $\delta = 692.2$ ppm with reference to $(CH_3)_2Te$ [16].

The ^{51}V static NMR spectra were measured at 105 MHz (9.4 T). A single pulse sequence was used: a pulse length of 1.0 μs, an accumulation of 400–800 scans and a pulse delay of 2.5 s for V_2O_5–TeO_2 glasses; a pulse length of 0.5 μs, an accumulation of 80–160 scans and a pulse

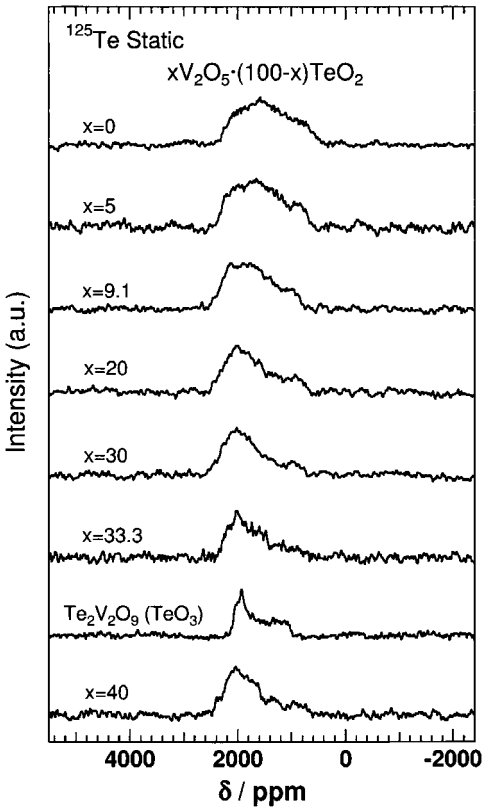

Figure 1. ^{125}Te static NMR spectra of $xV_2O_5{\cdot}(100-x)TeO_2$ glasses ($x = 0$, 5, 9.1, 20, 30, 33.3 and 40) and $Te_2V_2O_9$ crystal.

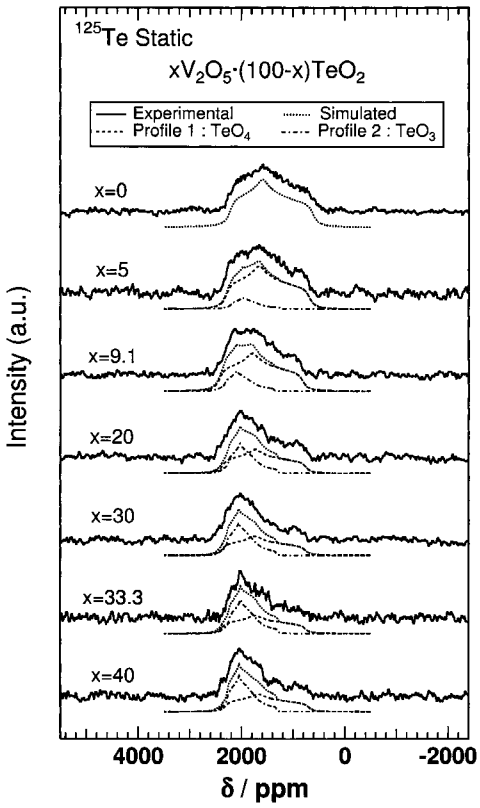

Figure 2. Simulated and experimental ^{125}Te static NMR spectra of $xV_2O_5{\cdot}(100-x)TeO_2$ glasses ($x = 0$, 5, 9.1, 20, 30, 33.3 and 40).

delay of 2.5 s for the $Te_2V_2O_9$ and $NaVTeO_5$ crystals. $Zn_3(VO_4)_2$ was used as a secondary standard, whose chemical shift is $\delta = -522$ ppm with reference to a $VOCl_3$ neat liquid [17].

2.4. ^{125}Te and ^{51}V static NMR spectral analyses

The principal components of the chemical shift tensors δ_1, δ_2 and δ_3 were estimated by fitting the theoretically calculated NMR spectra to the experimental NMR spectra, as described in the previous paper [15]. The isotropic chemical shift δ_{iso}, the chemical shift anisotropy $\Delta\delta$ and the asymmetry parameter η were also determined according to the following definitions [18, 19]:

$$\delta_{iso} = \frac{\delta_1 + \delta_2 + \delta_3}{3} \tag{1}$$

$$\Delta\delta = \delta_3 - \frac{\delta_1 + \delta_2}{2} \tag{2}$$

$$\eta = \frac{\delta_2 - \delta_1}{\delta_3 - \delta_{iso}}. \tag{3}$$

The principal components of the chemical shift tensors can be determined based on equation (4):

$$|\delta_3 - \delta_{iso}| \geqslant |\delta_1 - \delta_{iso}| \geqslant |\delta_2 - \delta_{iso}|. \tag{4}$$

3. Results

The analysed V^{4+}/V_{total} ratios are given in table 1. The experimental uncertainty in the V^{4+}/V_{total} values is $\pm 0.2\%$. The V^{4+}/V_{total} ratio increased up to 30 mol% V_2O_5 and then decreased with a further increase of V_2O_5 content. The latter tendency was consistent with a tendency already reported [4]. Since the fraction of V^{4+} ions is at most 6.9%, as given in table 1, the coordination state of V^{4+} ions seems negligible in discussion.

Table 2. Chemical shift parameters δ_1, δ_2, δ_3 and δ_{iso} used in simulation of ^{125}Te static NMR spectra, chemical shift anisotropy $\Delta\delta$ and asymmetry parameter η.

Glass	Profile 1: TeO_4						
x (mol%)	δ_1	δ_2	δ_3	δ_{iso}	$\Delta\delta$	η	Area (%)
TeO_2	2220	1590	620	1477	−1285	0.74	100
$xV_2O_5\cdot(100-x)TeO_2$							
$x = 5$	2290	1660	690	1547	−1285	0.74	89
$x = 9.1$	2420	1790	820	1677	−1285	0.74	81
$x = 20$	2360	1730	760	1617	−1285	0.74	64
$x = 30$	2370	1740	770	1627	−1285	0.74	57
$x = 33.3$	2370	1740	770	1627	−1285	0.74	55
$x = 40$	2310	1680	710	1567	−1285	0.74	53
	Profile 2: TeO_3						
	δ_1	δ_2	δ_3	δ_{iso}	$\Delta\delta$	η	Area (%)
TeO_2	—	—	—	—	—	—	0
$xV_2O_5\cdot(100-x)TeO_2$							
$x = 5$	2170	1980	1290	1813	−835	0.38	11
$x = 9.1$	2290	2100	1410	1933	−835	0.38	19
$x = 20$	2220	2030	1340	1863	−835	0.38	36
$x = 30$	2250	2060	1370	1893	−835	0.38	43
$x = 33.3$	2210	2020	1330	1853	−835	0.38	45
$x = 40$	2240	2050	1360	1883	−835	0.38	47

The δ_1, δ_2, δ_3, δ_{iso} and $\Delta\delta$ values have a unit of ppm. The errors in δ_1, δ_2 and δ_3 are ± 10 ppm. The errors in area are $\pm 2\%$.

Figure 1 shows the ^{125}Te static NMR spectra of V_2O_5–TeO_2 glasses and a $Te_2V_2O_9$ crystal. All spectra of glasses consisted of one broad peak without splitting in the range of 500 to 2800 ppm. The peak intensities in the range of 500–1800 ppm decreased with increasing V_2O_5 content, suggesting that the local structures around Te atoms change with the V_2O_5 content. The line profiles of a glass and a crystal with the $33.3V_2O_5\cdot 66.7TeO_2$ composition were quite different, indicating that the local structures around Te atoms are largely different between the two. In a similar manner as that in alkali tellurite glasses [10], the ^{125}Te static NMR spectra of V_2O_5–TeO_2 glasses were deconvoluted by using two spectral components: profile 1 due to TeO_4 tbp and profile 2 due to TeO_3 tp. Line profile deconvolutions are shown in figure 2. The values obtained by the spectral deconvolution are summarized in table 2. As for glasses containing more than 50 mol% V_2O_5, static spectra with S/N ratios adequate to perform the line profile deconvolution could not be obtained.

Figure 3 plots the TeO_4 tbp and TeO_3 tp fractions N_4 and N_3 against the M_yO content in M_yO–TeO_2 glasses (M = V, Li, Pb and Ga), where $xV_2O_5\cdot(100-x)TeO_2$ ($x = 5$, 9.1, 20, 30, 33.3 and 40) is converted into $x'V_{2/5}O\cdot(100-x')TeO_2$ ($x' = 20.8$, 33.3, 55.6, 68.2, 71.4 and 76.9), respectively. The experimental uncertainties in the N_3 and N_4 values are $\pm 2\%$. The N_3 value increases and the N_4 value decreases monotonically with increasing M_yO content.

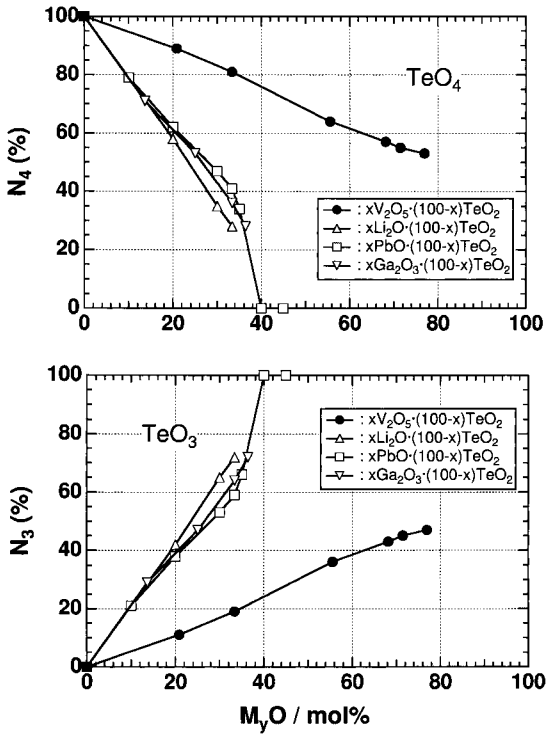

Figure 3. Plots of fractions of N_4 and N_3 against M_yO content in M_yO–TeO_2 glasses (M = V, Li, Pb and Ga).

The degree of increase of N_3 in the V_2O_5–TeO_2 glass system is much smaller than that in other tellurite glasses referred to in figure 3, indicating that the structures of V_2O_5–TeO_2 glasses are quite different from those of other tellurite glasses [10–12].

Figure 4 shows the ^{51}V static NMR spectra of V_2O_5–TeO_2 glasses together with those of the $Te_2V_2O_9$ and $NaVTeO_5$ crystals. The $NaVTeO_5$ [20] and $Te_2V_2O_9$ [21] crystals contain only a VO_4 tetrahedron and only a VO_5 tbp, respectively, as the structural unit. The static spectrum of $NaVTeO_5$ consists of one broad peak without splitting in the range of -350 to -800 ppm and has the strongest intensity at -520 ppm, while that of $Te_2V_2O_9$ is in the range of -200 to -1000 ppm and has the strongest intensity at -350 ppm (see table 3). Since the line profiles of the static spectra of these crystals gave typical powder patterns determined by the principal components of the chemical shift tensors δ'_1, δ'_2 and δ'_3, the δ'_1, δ'_2 and δ'_3 values can be estimated from the spectra. The isotropic chemical shift δ'_{iso}, the chemical shift anisotropy $\Delta\delta'$ and the asymmetry parameter η' were calculated using equations (1)–(3). The results are listed in table 3. Figure 5 shows the relationship between the asymmetry parameter η' and the absolute value of the chemical shift anisotropy $|\Delta\delta'|$ for various structural units found in various vanadate glasses and crystals [13, 14, 22].

On the other hand, all the static spectra of V_2O_5–TeO_2 glasses consist of two broad peaks in the range of -1400 to 300 ppm and have long tails extending to low frequencies, indicating that the glasses consist of both VO_4 tetrahedra and VO_5 tbp in the whole composition range. On the basis of the line profiles of $NaVTeO_5$ and $Te_2V_2O_9$ crystals, peaks around -500 and -280 ppm in the V_2O_5–TeO_2 glasses can be assigned to VO_4 tetrahedra and VO_5 tbp, respectively, and long tails extending to low frequencies are due to VO_5 tbp. The experimental ^{51}V static NMR

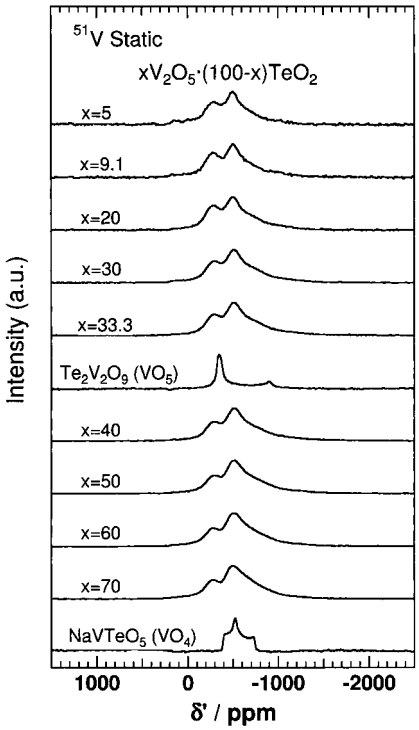

Figure 4. ^{51}V static NMR spectra of $x\mathrm{V_2O_5}\cdot(100-x)\mathrm{TeO_2}$ glasses ($x = 5, 9.1, 20, 30, 33.3, 40, 50, 60$ and 70) and $\mathrm{Te_2V_2O_9}$ and $\mathrm{NaVTeO_5}$ crystals.

spectra were deconvoluted by using two spectral components: peak 1 due to VO_4 tetrahedra and peak 2 due to VO_5 tbp. Line profile deconvolutions performed are shown in figure 6. The δ'_1, δ'_2, δ'_3, δ'_{iso}, $\Delta\delta'$ and η' values obtained are summarized in table 3. The NMR parameters η' and $|\Delta\delta'|$ of peaks 1 and 2 are shown in figure 5.

The $(V_2O_8)_n$ zigzag chain in figure 5 consists of VO_5 tbp, and the VO_4^{3-}, $V_2O_7^{4-}$ and $(VO_3)_n^{n-}$ chain consist only of VO_4 tetrahedra. If the $|\Delta\delta'|$ values of vanadate glasses and crystals are less than 450 ppm or more than 550 ppm, then the constituting structural units can be undoubtedly regarded as VO_4 tetrahedra and VO_5 tbp, respectively. The $|\Delta\delta'|$ values of $NaVTeO_5$ and $Te_2V_2O_9$ are 289 and 609 ppm, respectively, indicating that the classification described above is reasonable. All the values of peak 1 are less than 450 ppm in $|\Delta\delta'|$, while those of peak 2 are more than 800 ppm. This result verifies that peaks 1 and 2 correspond to VO_4 tetrahedron and VO_5 tbp, respectively.

Figure 7 plots the VO_4 tetrahedron and VO_5 tbp fractions N'_4 and N'_5 against the V_2O_5 content in the V_2O_5–TeO_2 glasses. The experimental uncertainties in the N'_4 and N'_5 values are $\pm 1\%$. The N'_4 value increases and the N'_5 value decreases up to $\sim$40 mol% V_2O_5 and then the degree of changes in N'_4 and N'_5 becomes small with a further increase in V_2O_5 content.

4. Discussion

4.1. Local structure of V_2O_5–TeO_2 *glasses*

The highest absorption bands at 940–1000 cm^{-1} in the infrared spectra of V_2O_5–TeO_2 glasses [9] are assigned to V=O double bonds. Therefore, the V=O double bonds are considered to be contained as the structural units of vanadate groups in the V_2O_5–TeO_2 glasses. Figure 8

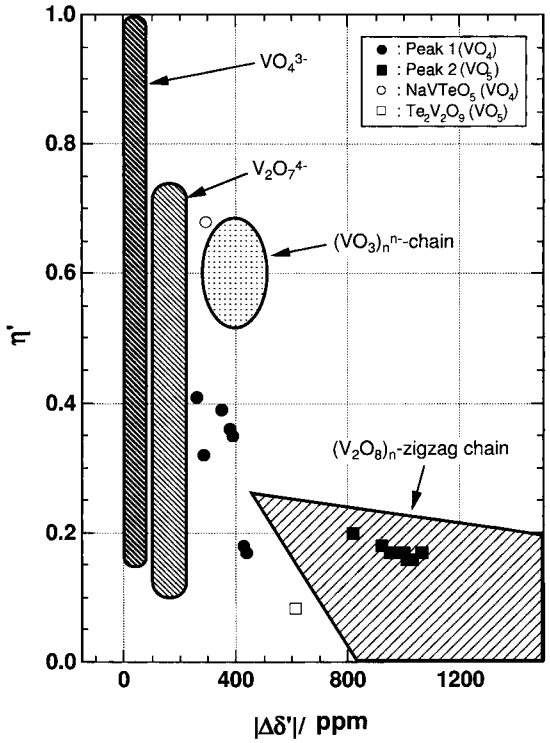

Figure 5. Plots of η' against $|\Delta\delta'|$ for V_2O_5–TeO_2 glasses and $NaVTeO_5$ and $Te_2V_2O_9$ crystals.

shows the structural units of VO_4 tetrahedra and VO_5 tbps which are probably contained in the V_2O_5–TeO_2 glasses in a manner similar to several vanadate crystals [20, 21, 23, 24, 26].

The VO_4 tetrahedra are classified into three groups: (i) VO_4^{3-}, (ii) $V_2O_7^{4-}$ and (iii) $(VO_3)_n^{n-}$ chains. The VO_4^{3-} has two V=O double bonds and the $V_2O_7^{4-}$ and $(VO_3)_n^{n-}$ chain have one V=O double bond per V atom. The VO_4^{3-}, $V_2O_7^{4-}$ and $(VO_3)_n^{n-}$ chain are found in the $NaVTeO_5$ [20], $Mg_2V_2O_7$ [23] and $LiVO_3$ crystals [24], respectively. The structure of VO_4^{3-} in $NaVTeO_5$ is quite different from that in divalent-metal orthovanadate crystals such as $Ba_3(VO_4)_2$ [25]. Four regions determined by both η' and $|\Delta\delta'|$ of VO_4^{3-}, $V_2O_7^{4-}$, $(VO_3)_n^{n-}$ chain and $(V_2O_8)_n$ zigzag chain in monovalent-metal and divalent-metal vanadate crystals and glasses are depicted in figure 5. Therefore, the point determined by both $|\Delta\delta'|$ and η' of $NaVTeO_5$ is not located in the region of VO_4^{3-} as illustrated in figure 5.

The VO_5 tbps are classified into two groups: (i) $(VO_4)_n^{3n-}$ chains and (ii) $(V_2O_8)_n$ zigzag chains. The former is found in a $Te_2V_2O_9$ crystal [21], while the latter in a β-$NaVO_3$ crystal [26]. Both groups have one V=O double bond per V atom.

The composition dependence of $|\Delta\delta'|$ of VO_4 tetrahedra in the V_2O_5–TeO_2 glasses is shown in figure 9. The broken line in this figure denotes the $|\Delta\delta'|$ value (289 ppm) of VO_4 tetrahedra in an $NaVTeO_5$ crystal containing only VO_4^{3-}. The $|\Delta\delta'|$ of V_2O_5–TeO_2 glasses increase with increasing V_2O_5 content. Since the $|\Delta\delta'|$ values of glasses containing 5 and 9.1 mol% V_2O_5 are smaller than that of an $NaVTeO_5$ crystal, it can be deduced that VO_4^{3-} is mainly formed in these glasses. From the four regions determined by both η' and $|\Delta\delta'|$ of VO_4^{3-}, $V_2O_7^{4-}$ and $(VO_3)_n^{n-}$ chain (figure 5), the following order in $|\Delta\delta'|$ is found: $(VO_3)_n^{n-}$ chain $> V_2O_7^{4-} > VO_4^{3-}$. The $|\Delta\delta'|$ values of glasses with more than 20 mol% V_2O_5 are much

Table 3. Chemical shift parameters δ'_1, δ'_2, δ'_3 and δ'_{iso} used in simulation of ^{51}V static NMR spectra, chemical shift anisotropy $\Delta\delta'$ and asymmetry parameter η'.

Glass	Peak 1: VO_4						
x (mol%)	δ'_1	δ'_2	δ'_3	δ'_{iso}	$\Delta\delta'$	η'	Area (%)
$xV_2O_5{\cdot}(100-x)TeO_2$							
$x = 5$	−430	−500	−720	−550	−255	0.41	25
$x = 9.1$	−440	−500	−750	−563	−280	0.32	28
$x = 20$	−410	−500	−800	−570	−345	0.39	34
$x = 30$	−420	−510	−840	−590	−375	0.36	38
$x = 33.3$	−420	−510	−840	−590	−375	0.36	39
$x = 40$	−420	−510	−850	−593	−385	0.35	42
$x = 50$	−440	−490	−900	−610	−435	0.17	45
$x = 60$	−440	−490	−890	−607	−425	0.18	46
$x = 70$	−450	−500	−900	−617	−425	0.18	48
$NaVTeO_5$*	−389	−520	−743	−551	−289	0.68	—
$Te_2V_2O_9$*	—	—	—	—	—	—	—
	Peak 2: VO_5						
	δ'_1	δ'_2	δ'_3	δ'_{iso}	$\Delta\delta'$	η'	Area (%)
$xV_2O_5{\cdot}(100-x)TeO_2$							
$x = 5$	−170	−280	−1040	−497	−815	0.20	75
$x = 9.1$	−170	−280	−1140	−530	−915	0.18	72
$x = 20$	−170	−280	−1180	−543	−955	0.17	66
$x = 30$	−170	−280	−1170	−540	−945	0.17	62
$x = 33.3$	−180	−290	−1230	−567	−995	0.17	61
$x = 40$	−170	−280	−1220	−557	−995	0.17	58
$x = 50$	−160	−280	−1280	−573	−1060	0.17	55
$x = 60$	−160	−270	−1220	−550	−1005	0.16	54
$x = 70$	−160	−270	−1240	−557	−1025	0.16	52
$NaVTeO_5$*	—	—	—	—	—	—	—
$Te_2V_2O_9$*	−316	−350	−942	−536	−609	0.08	—

The δ'_1, δ'_2, δ'_3, δ'_{iso} and $\Delta\delta'$ values have a unit of ppm. Asterisks denote vanadate crystals. The errors in δ'_1, δ'_2 and δ'_3 in V_2O_5–TeO_2 glasses and vanadate crystals are ±10 ppm and ±1 ppm respectively. The errors in area are ±1%.

larger than that of an $NaVTeO_5$ crystal, suggesting that the size of $(VO_3)_n^{n-}$ chains increases with increasing V_2O_5 content.

4.2. Possible linkage modes between tellurite structural units and vanadate structural units

According to the structural model previously proposed [10–12], three tellurite structural units, $TeO_{4/2}$ (TeO_4 tbp without a non-bridging oxygen (NBO)), $O_{3/2}Te–O^-$ (TeO_4 tbp with an NBO) and $O_{1/2}Te(=O)–O^-$ (TeO_3 tp with two NBOs), are considered to be formed in V_2O_5–TeO_2 glasses when the V_2O_5 contents are small. As is well known, TeO_4 tbp contains two kinds of bonds: two Te–O_{ax} bonds and two Te–O_{eq} bonds. The Te–O_{ax} bonds are longer than Te–O_{eq} bonds. The difference in bond distance is considered to correspond to that in bond valence (BV). For example, the BV of Te–O bonds can be estimated using the following equation given by Philippot [27]:

$$\mathrm{BV} = 1.333(r/0.1854)^{-5.2} \tag{5}$$

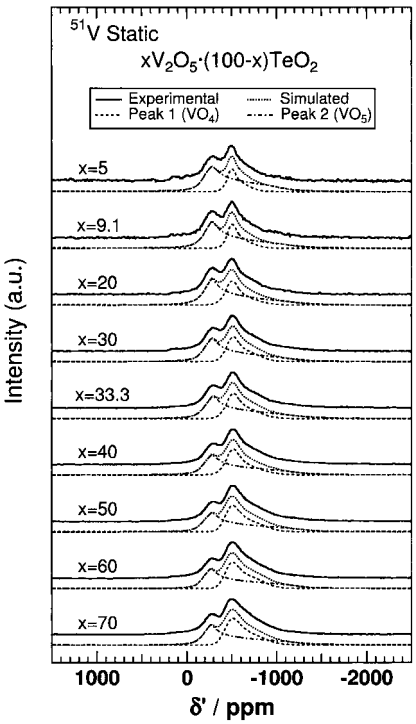

Figure 6. Simulated and experimental ^{51}V static NMR spectra of $x\mathrm{V_2O_5}\cdot(100-x)\mathrm{TeO_2}$ glasses ($x = 5$, 9.1, 20, 30, 33.3, 40, 50, 60 and 70).

where r is the Te–O distance in nm. Since the Te–O_{ax} and Te–O_{eq} bond distances of TeO_4 tbp in several tellurite crystals take the values of 0.204–0.219 and 0.183–0.195 nm [15], respectively, equation (5) gives BV = 0.81–0.56 and 1.43–1.03. Although weak Te–O bonds with distances longer than 0.25 nm are usually ignored, it should be kept in mind that weak interactions between two atoms are effectively not zero. A difference in BV between the Te–O_{ax} bond and the Te–O_{eq} bond in TeO_4 tbp in representative tellurite crystals is 0.24–0.73. If a difference in BV between the Te–O_{ax} bond and the Te–O_{eq} bond in TeO_4 tbp is 0.24–0.73, therefore, it can be undoubtedly deduced that such a TeO_4 tbp is stable. An additional assumption that a TeO_4 tbp consists of two equivalent Te–O_{ax} bonds and two equivalent Te–O_{eq} bonds was made in order to simplify the present model. Since the Te–O_{NBO} bond distances in $O_{1/2}Te(=O)–O^-$ in several tellurite crystals take the value of 0.183–0.1862 nm [15], equation (5) gives BV = 1.43–1.30.

The possible linkage modes between $O_{1/2}Te(=O^-)$–O sharing an edge with VO_4^{3-} or a $(VO_4)_n^{3n-}$ chain and TeO_4 tbp sharing its corner are shown in figure 10. The numerals in this figure indicate the BV values which were calculated based on an assumption described below. The VO_4^{3-} has two V=O double bonds and two V–O_{NBO} bonds. The VO_5 tbps in the $(VO_4)_n^{3n-}$ chain have one V=O double bond, two V–O_{BO} and two V–O_{NBO} bonds, where O_{BO} and O_{NBO} denote a bridging oxygen (BO) and a non-bridging oxygen (NBO). The BV values of V=O double bonds and V–O_{BO} bonds are assumed to be 2 and 1, respectively, because of the twofold coordinated O_{BO}. Since the V–O_{NBO} bonds in VO_4^{3-} and $(VO_4)_n^{3n-}$ chains in vanadate crystals have almost the same distances [20, 21], it seems reasonable to assume that the V–O_{NBO} bonds in VO_4^{3-} and $(VO_4)_n^{3n-}$ chains are equivalent and have the same BV values of 0.5. Hence, the BV values of two Te–O bonds in the $O_{1/2}Te(=O)–O^-$ sharing an edge via two oxygens with VO_4^{3-} or a $(VO_4)_n^{3n-}$ chain become 1.5. As a result, the BV value of the Te–O bond in the $O_{1/2}Te(=O)–O^-$ sharing an oxygen with a TeO_4 tbp is 1.0. Therefore, the

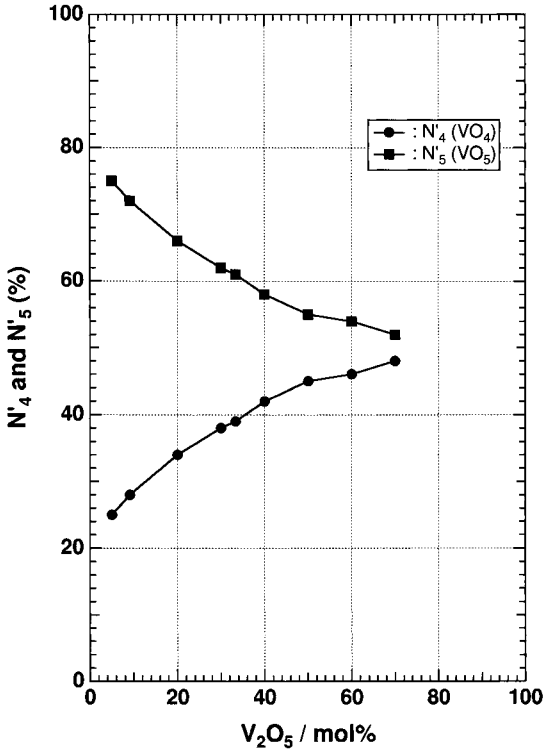

Figure 7. Plots of fractions of N_4' and N_5' against V_2O_5 content in V_2O_5–TeO_2 glasses.

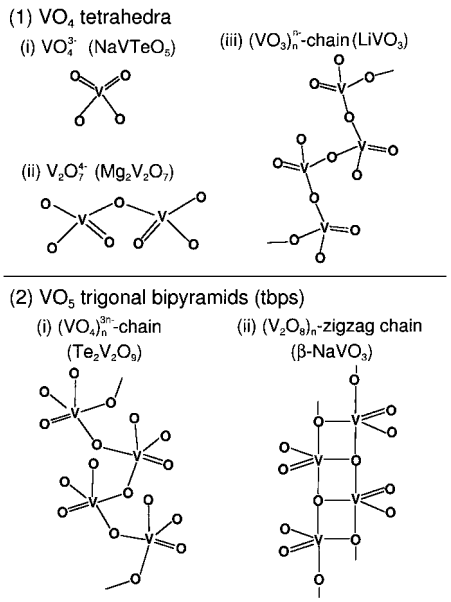

Figure 8. Structural units composed of VO_4 tetrahedra and VO_5 trigonal bipyramids (tbps) which are probably contained in V_2O_5–TeO_2 glasses.

BV values of Te–O_{ax} and Te–O_{eq} bonds in the TeO_4 tbp are 1.0. In this case the difference in bond valence BV(Te–O_{eq})-BV(Te–O_{ax}) between the Te–O_{ax} bond and Te–O_{eq} bond in the

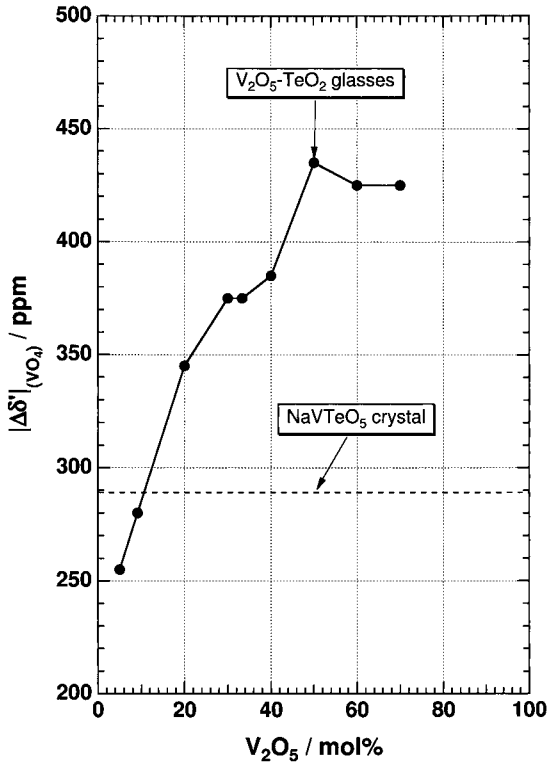

Figure 9. Composition dependence of $|\Delta\delta'|_{(VO_4)}$ of VO_4 tetrahedra in V_2O_5–TeO_2 glasses.

TeO_4 tbp is zero, suggesting that the TeO_4 tbp is unstable. The distances of V=O double bonds in vanadate crystals are not constant [20, 21, 23, 24, 26], indicating that the BV values of V=O double bonds in vanadate crystals are not constant. This means that the BV values of V=O bonds in vanadate crystals change depending on the environment around V=O bonds. Therefore, the BV values of V=O bonds in V_2O_5–TeO_2 glasses may be also changed depending on the environment around V=O bonds. If a fraction of the BV of V=O bonds in VO_4^{3-} or $(VO_4)_n^{3n-}$ chains (for example, 0.15) is transferred to the BV of V–O_{NBO} bonds, the BVs take values as shown in parentheses in figure 10. In this case the BV(Te–O_{eq})-BV(Te–O_{ax}) values become 0.6 and 0.3 in VO_4^{3-} and $(VO_4)_n^{3n-}$ chains, respectively, and then the TeO_4 tbp becomes stable.

Possible linkage modes of corner sharing between $V_2O_7^{4-}$, a $(VO_3)_n^{n-}$ chain or a $(V_2O_8)_n$ zigzag chain and $O_{3/2}Te$–$_{ax}O^-$ are illustrated in figure 11. The numerals in this figure have the same meaning as those in figure 10. The VO_4 tetrahedra in $(VO_3)_n^{n-}$ chains are composed of one V=O double bond, two V–O_{BO} bonds and one V–O_{NBO} bond. The BV values of the V–O_{NBO} bonds are estimated to be 1 based on the assumption already mentioned. Since $V_2O_7^{4-}$ corresponds to a $(VO_3)_n^{n-}$ chain with $n = 2$, the BV values of V–O_{NBO} bonds in $V_2O_7^{4-}$ are also estimated to be 1. The VO_5 tbps in $(V_2O_8)_n$ zigzag chains consist of one V=O double bond, three V–O_{BO} bonds and one V–O_{NBO} bond. The BV values of the V–O_{BO} bonds in $(V_2O_8)_n$ zigzag chains are assumed to be 2/3 because of the threefold coordinated O_{BO}. Therefore, the BV value of a V–O_{NBO} bond in a $(V_2O_8)_n$ zigzag chain is estimated to be 1. The BV values of two Te–O_{ax} bonds in the TeO_4 tbp sharing its axial oxygen with one of $V_2O_7^{4-}$, a $(VO_3)_n^{n-}$

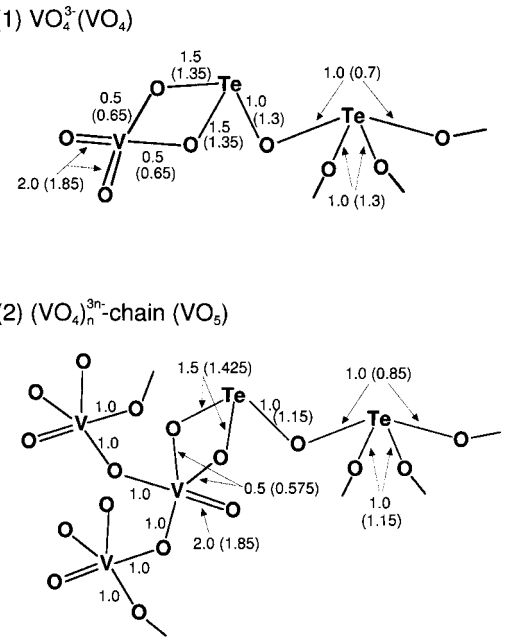

Figure 10. Possible linkage modes of corner sharing between edge-shared $O_{1/2}Te(=O)–O^-$ with VO_4^{3-} or a $(VO_4)^{3n-}$ chain and TeO_4 tbp.

chain or a $(V_2O_8)_n$ zigzag chain become 1. As a result the BV values of two Te–O_{eq} bonds in the TeO_4 tbp are also 1. In this case BV(Te–O_{eq})-BV(Te–O_{ax}) becomes zero, so that the $O_{3/2}Te–_{ax}O^-$ is unstable. If a fraction of the BV of V=O bonds in $V_2O_7^{4-}$, $(VO_3)_n^{n-}$ chains or $(V_2O_8)_n$ zigzag chains (for example, 0.3 for $V_2O_7^{4-}$, 0.15 for $(VO_3)_n^{n-}$ chains or $(V_2O_8)_n$ zigzag chains) is transferred to the BV of V–O_{NBO} bonds as shown in figure 11, the BVs take the values in parentheses. In this case, BV(Te–O_{eq})-BV(Te–O_{ax}) is 0.3 and then the TeO_4 tbp becomes stable. Since the BVs of the Te–O_{eq} bond in $O_{3/2}Te–_{eq}O^-$ and the Te–O_{NBO} bonds in $O_{1/2}Te(=O)–O^-$ are larger than unity, both $O_{3/2}Te–_{eq}O^-$ and $O_{1/2}Te(=O)–O^-$ would not be connected with $V_2O_7^{4-}$, $(VO_3)_n^{n-}$ chains and $(V_2O_8)_n$ zigzag chains.

Therefore, it can be concluded that VO_4^{3-} and $(VO_4)_n^{3n-}$ chains are preferentially linked with $O_{1/2}Te(=O)–O^-$ by sharing their edges, whereas $V_2O_7^{4-}$, $(VO_3)_n^{n-}$ chains and $(V_2O_8)_n$ zigzag chains are preferentially linked with $O_{3/2}Te–_{ax}O^-$.

4.3. Structure model of V_2O_5–TeO_2 *glasses*

In our previous papers [10–12], the fractions of $TeO_{4/2}$, $O_{3/2}Te–O^-$ and $O_{1/2}Te(=O)–O^-$ were calculated by using a model of a structural change. The fractions can be quantitatively calculated using the model only when all the oxygen atoms in metal oxides other than TeO_2 are completely used to break a Te–O–Te linkage. Hence, the fractions cannot be quantitatively obtained using the model in V_2O_5–TeO_2 glasses since the V–O–V linkages as seen in $(V_2O_8)_n$ zigzag chains and the V=O double bonds are contained in the glasses (see figure 5).

The numbers of NBO atoms in the tellurite and vanadate structural units, which can be calculated from the fractions of the structural units and glass compositions, are used in considering the tellurite and vanadate structural units at each glass composition in V_2O_5–TeO_2 glasses. ΣMO_n (the numbers of MO_n polyhedra (TeO_3 tp, TeO_4 tbp, VO_4 tetrahedra and

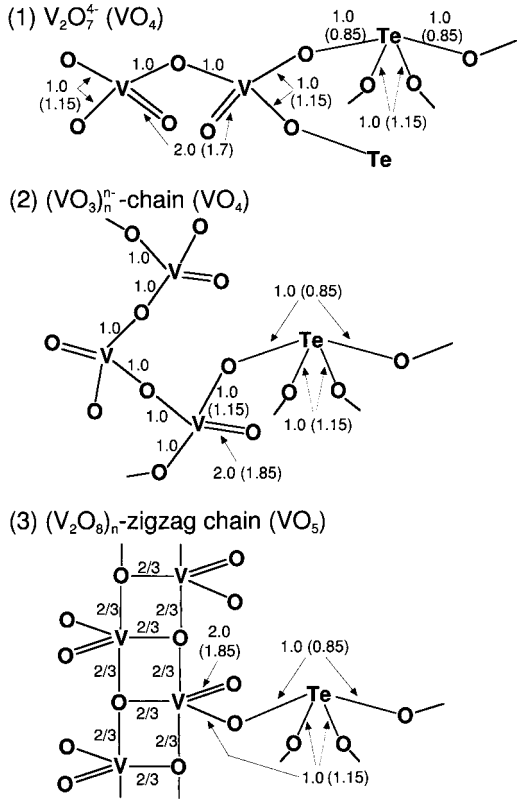

Figure 11. Possible linkage modes of corner sharing between $V_2O_7^{4-}$, a $(VO_3)_n^{n-}$ chain or a $(V_2O_8)_n$ zigzag chain and $O_{3/2}Te$–$_{ax}O^-$.

VO_5 tbp) per unit chemical formula) and ΣO_{NBO} (the numbers of NBO atoms in the present structural units) were calculated on the basis of glass compositions. ΣMO_n and ΣO_{NBO} are listed in table 4. According to the previous structural model [10–12], three tellurite structural units $TeO_{4/2}$, $O_{3/2}Te$–O^- and $O_{1/2}Te(=O)$–O^- probably exist when the V_2O_5 content is small. In this case the numbers of NBO atoms in $O_{1/2}Te(=O)$–O^-, VO_4 and VO_5 can be calculated, but the fraction of $O_{3/2}Te$–O^- units is not known. Almost all the NBO atoms in vanadate structural units are considered to be connected with Te atoms. On the basis of this assumption, the fraction of $O_{3/2}Te$–O^- is estimated from the numbers of NBO atoms in $O_{1/2}Te(=O)$–O^-, VO_4 and VO_5.

Since $V_2O_7^{4-}$ corresponds to a $(VO_3)_n^{n-}$ chain with $n = 2$, it can be regarded as a species of $(VO_3)_n^{n-}$ chain. The procedure in the estimation of the fractions of $O_{3/2}Te$–O^- units is as follows:

ΣO_{NBO} of a structural unit can be calculated from the following equation and procedures.

$$\Sigma O_{NBO} = \Sigma MO_n \times (\text{the fraction of a structural unit in } MO_n \text{ polyhedra}) \times (\text{the numbers of NBOs per cation in a structural unit}). \quad (6)$$

(i) The numbers of NBOs of $O_{1/2}Te(=O)$–O^- ($\Sigma O_{NBO}(O_{1/2}Te(=O)$–$O^-)$) are calculated. Here all the TeO_3 tps are assumed to be $O_{1/2}Te(=O)$–O^-.

(ii) The numbers of NBOs of $(VO_4)_n^{3n-}$ chains ($\Sigma O_{NBO}((VO_4)_n^{3n-}$ chain (100%))) are calculated, when all the VO_5 tbps consist of $(VO_4)_n^{3n-}$ chains.

Table 4. ΣMO_n (numbers of MO_n polyhedra (TeO_3, TeO_4, VO_4 and VO_5) per unit chemical formula) and ΣO_{NBO} (numbers of non-bridging oxygen (NBO) atoms in structural units), which were obtained by ^{51}V and ^{125}Te static NMR measurements.

Glass composition (mol%)	ΣMO_n[a]		ΣO_{NBO}	
$5V_2O_5{\cdot}95TeO_2$	VO_4 (25%)	2.5	VO_4^{3-} (2^b, $TeO_3{}^c$) → 5	(100% in VO_4)
	VO_5 (75%)	7.5	$(VO_4)_n^{3n-}$ chain (2^b, $TeO_3{}^c$) → 15	(100% in VO_5)
	TeO_4 (89%)	84.5	$TeO_{4/2}$ (0^b) → 0	(100% in TeO_4)
			$O_{3/2}Te–O^-$ (1^b) → 0	(0% in TeO_4)
	TeO_3 (11%)	10.5	$O_{1/2}Te(=O–O^-$ (2^b) → 21	(100% in TeO_3)
$9.1V_2O_5{\cdot}90.9TeO_2$	VO_4 (28%)	5.1	VO_4^{3-} (2^b, $TeO_3{}^c$) → 8.4	(82% in VO_4)
			$(VO_3)_n^{n-}$ chain (1^b, $TeO_4{}^c$) → 0.9	(18% in VO_4)
	VO_5 (72%)	13.1	$(VO_4)_n^{3n-}$ chain (2^b, $TeO_3{}^c$) → 26.2	(100% in VO_5)
	TeO_4 (81%)	73.6	$TeO_{4/2}$ (0^b) → 0	(99% in TeO_4)
			$O_{3/2}Te–O^-$ (1^b) → 0.9	(1% in TeO_4)
	TeO_3 (19%)	17.3	$O_{1/2}Te(=O)–O^-$ (2^b) → 34.6	(100% in TeO_3)
$20V_2O_5{\cdot}80TeO_2$	VO_4 (34%)	13.6	VO_4^{3-} (2^b, $TeO_3{}^c$) → 4.8	(18% in VO_4)
			$(VO_3)_n^{n-}$ chain (1^b, $TeO_4{}^c$) → 11.2	(82% in VO_4)
	VO_5 (66%)	26.4	$(VO_4)_n^{3n-}$ chain (2^b, $TeO_3{}^c$) → 52.8	(100% in VO_5)
	TeO_4 (64%)	51.2	$TeO_{4/2}$ (0^b) → 0	(78% in TeO_4)
			$O_{3/2}Te–O^-$ (1^b) → 11.2	(22% in TeO_4)
	TeO_3 (36%)	28.8	$O_{1/2}Te(=O)–O^-$ (2^b) → 57.6	(100% in TeO_3)
$30V_2O_5{\cdot}70TeO_2$	VO_4 (38%)	22.8	$(VO_3)_n^{n-}$ chain (1^b, $TeO_4{}^c$) → 22.8	(100% in VO_4)
	VO_5 (62%)	37.2	$(VO_4)_n^{3n-}$ chain (2^b, $TeO_3{}^c$) → 60.2	(81% in VO_5)
			$(V_2O_8)_n$ zigzag chain (1^b, $TeO_4{}^c$) → 7.1	(19% in VO_5)
	TeO_4 (57%)	39.9	$TeO_{4/2}$ (0^b) → 0	(25% in TeO_4)
			$O_{3/2}Te–O^-$ (1^b) → 29.9	(75% in TeO_4)
	TeO_3 (43%)	30.1	$O_{1/2}Te(=O)–O^-$ (2^b) → 60.2	(100% in TeO_3)
$33.3V_2O_5{\cdot}66.7TeO_2$	VO_4 (39%)	26.0	$(VO_3)_n^{n-}$ chain (1^b, $TeO_4{}^c$) → 26.0	(100% inVO_4)
	VO_5 (61%)	40.6	$(VO_4)_n^{3n-}$ chain (2^b, $TeO_3{}^c$) → 60.0	(74% in VO_5)
			$(V_2O_8)_n$ zigzag chain (1^b, $TeO_4{}^c$) → 10.6	(26% in VO_5)
	TeO_4 (55%)	36.7	$TeO_{4/2}$ (0^b) → 0	(0.3% in TeO_4)
			$O_{3/2}Te–O^-$ (1^b) → 36.6	(99.7% in TeO_4)
	TeO_3 (45%)	30.0	$O_{1/2}Te(=O)–O^-$ (2^b) → 60.0	(100% in TeO_3)

[a] ΣMO_n = (total number of Te or V per unit chemical formula) × (fraction of MO_n polyhedra).
[b] The numeral in parentheses is the number of NBO per cation in a structural unit.
[c] A vanadate structural unit is preferentially linked with the corresponding tellurite structural unit in parentheses.

(iii) (a) When $\Sigma O_{NBO}(O_{1/2}Te(=O)–O^-) > \Sigma O_{NBO}((VO_4)_n^{3n-}$ chain (100%)) ($V_2O_5 \leqslant$ 20 mol%), the numbers of NBOs of VO_4^{3-} ($\Sigma O_{NBO}(VO_4^{3-})$) can be estimated by the following equation:

$$\Sigma O_{NBO}(VO_4^{3-}) = \Sigma O_{NBO}(O_{1/2}Te(=O)–O^-) - \Sigma O_{NBO}((VO_4)_n^{3n-}\text{chain}(100\%)). \quad (7)$$

In this case the numbers of NBOs of $(VO_4)_n^{3n-}$ chains ($\Sigma O_{NBO}((VO_4)_n^{3n-}$ chain)) become equal to ΣO_{NBO} ($(VO_4)_n^{3n-}$ chain (100%)). In a $5V_2O_5{\cdot}95TeO_2$ glass where all the VO_4 tetrahedra are considered to be VO_4^{3-}, ΣO_{NBO} (VO_4^{3-}) is estimated to be 5 since ΣO_{NBO} (VO_4^{3-}) is 5 and is small compared with ΣO_{NBO} (VO_4^{3-}) obtained by equation (7).

(b) The fractions of VO_4^{3-} and $(VO_3)_n^{3n-}$ chains in VO_4 tetrahedra are obtained.

(c) The numbers of NBOs of $(VO_3)_n^{n-}$ chains ($\Sigma O_{NBO}((VO_3)_n^{n-}$ chain)) are estimated.

(d) The numbers of NBOs of $O_{3/2}Te–O^-$ ($\Sigma O_{NBO}(O_{3/2}Te–O^-)$) become equal to that of $(VO_3)_n^{n-}$ chains since $O_{3/2}Te–O^-$ is considered to be preferentially connected with

$(VO_3)_n^{n-}$ chains as mentioned above.

(iv) (a) When $\Sigma O_{NBO}((VO_4)_n^{3n-}$ chain (100%)) $> \Sigma O_{NBO}(O_{1/2}Te(=O)–O^-)$ in glasses with $30 \leqslant V_2O_5 \leqslant 33.3$ mol%, the numbers of NBOs of $(VO_4)_n^{3n-}$ chains ($\Sigma O_{NBO}((VO_4)_n^{3n-}$ chain)) are equal to that of $O_{1/2}Te(=O)–O^-$.

(b) The fractions of $(VO_4)_n^{3n-}$ chains and $(V_2O_8)_n$ zigzag chains in VO_5 tbp are obtained.

(c) The numbers of NBOs of $(V_2O_8)_n$ zigzag chains ($\Sigma O_{NBO}(V_2O_8)_n$ zigzag chain)) are estimated.

(d) $\Sigma O_{NBO}(O_{3/2}Te–O^-)$ is obtained as the summation of $\Sigma O_{NBO}((VO_3)_n^{n-}$ chain) and $\Sigma O_{NBO}((V_2O_8)_n$ zigzag chain).

(v) The fractions of $TeO_{4/2}$ and $O_{3/2}Te–O^-$ can be estimated from $\Sigma O_{NBO}(O_{3/2}Te–O^-)$.

Table 5. Fractions of tellurite and vanadate structural units in glasses containing V_2O_5 up to 33.3 mol%.

Glass	TeO_4 (%)		TeO_3 (%)	VO_4 (%)		VO_5 (%)	
x (mol%)	$TeO_{4/2}$	$O_{3/2}Te–O^-$	$O_{1/2}Te(=O)–O^-$	VO_4^{3-}	$(VO_3)_n^{n-}$ chain	$(VO_4)_n^{3n-}$ chain	$(V_2O_8)_n$ zigzag chain
TeO_2	100	0	0	—	—	—	—
$xV_2O_5{\cdot}(100-x)TeO_2$							
$x = 5$	89	0	11	25	0	75	0
$x = 9.1$	80	1	19	23	5	72	0
$x = 20$	50	14	36	6	28	66	0
$x = 30$	14	43	43	0	38	50	12
$x = 33.3$	0.2	54.8	45	0	39	45	16

The errors in the fractions of tellurite and vanadate structural units were calculated on the basis of the errors in area in tables 2 and 3.
The errors in the fractions of tellurite structural units are ±3%.
The errors in the fractions of VO_4 structural units in the glasses with 9.1 and 20 mol% V_2O_5 are ±11 and ±5%, respectively.
The errors in the fractions of VO_5 structural units in the glass with 30 and 33.3 mol% V_2O_5 are ±3%.
The errors in the fractions of other vanadate structural units are ±1%.

The fractions of tellurite and vanadate structural units in glasses containing V_2O_5 up to 33.3 mol% are shown in figure 12 and table 5. The error in the estimated $O_{3/2}Te–O^-$ fractions is at most ±3%. The errors in the estimated $(VO_4)_n^{3n-}$ chain and $(V_2O_8)_n$ zigzag chain fractions in the range of 30–33.3 mol% V_2O_5 are ±3%. The errors in the estimated VO_4^{3-} fractions in the range of 9.1–20 mol% V_2O_5 are ±5–11%. The $TeO_{4/2}$ fraction decreases, while the $O_{3/2}Te–O^-$ and $O_{1/2}Te(=O)–O^-$ fractions increase with increasing V_2O_5 content. The initial addition of V_2O_5 to TeO_2 glass results in the formation not of $O_{3/2}Te–O^-$ but of $O_{1/2}Te(=O)–O^-$, and the $O_{3/2}Te–O^-$ fraction increases rapidly above 20 mol% V_2O_5. This tendency is similar to that in other tellurite glasses investigated in the previous papers [10–12]. The VO_4^{3-} and $(VO_4)_n^{3n-}$ chain fractions decrease and the $(VO_3)_n^{n-}$ chain increases with increasing V_2O_5 content. The $(V_2O_8)_n$ zigzag chain fraction is 0% up to 20 mol% V_2O_5 and then increases with a further increase of V_2O_5 content. The $(VO_3)_n^{n-}$ chain, $(VO_4)_n^{3n-}$ chain and $(V_2O_8)_n$ zigzag chain are contained in glasses with V_2O_5 contents more than 30 mol%, suggesting that all the vanadate structural units act as a network former in the glasses.

Thus, both V_2O_5 and TeO_2 can act as a network formers in the V_2O_5–TeO_2 glasses. The tellurite structural units such as $TeO_{4/2}$ and $O_{3/2}Te–O^-$ mainly form a glass network in glasses with low V_2O_5 contents, while the vanadate structural units such as $(VO_3)_n^{n-}$ chains, $(VO_4)_n^{3n-}$ chains and $(V_2O_8)_n$ zigzag chains mainly form a glass network in glasses with high

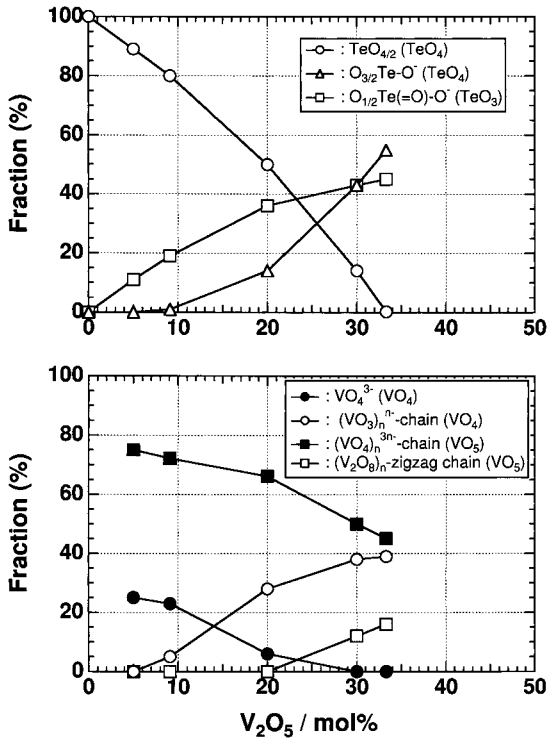

Figure 12. Plots of fractions of tellurite (upper figure) and vanadate (lower figure) structural units against compositions in V_2O_5–TeO_2 glasses containing V_2O_5 up to 33.3 mol%.

V_2O_5 contents. This can explain the reason whey the binary V_2O_5–TeO_2 system has a very wide glass-forming region.

As described above, the N_3 and N_4 values are different between the V_2O_5–TeO_2 glass system and other metal glass systems in the previous papers [10–12]. Probably this can be explained as follows. Because MO_n polyhedra (M = alkali metal, Mg, Zn, Sr, Ba, Pb, Al and Ga) in the glasses do not form a glass network by themselves and M cations exist as free ions, all the oxygen atoms in these metal oxides are completed used to break Te–O–Te linkages. Since V–O–V linkages seen in $(VO_3)_n^{n-}$, $(VO_4)_n^{3n-}$ and $(V_2O_8)_n$ chains and V=O double bonds are contained in V_2O_5–TeO_2 glasses, on the other hand, not all the oxygen atoms in V_2O_5 added to tellurite glass are used to break Te–O–Te linkages, in other words, to form TeO_3 tp. Even if the number of oxygen atoms in the metal oxides added to tellurite glass is equal, therefore, the numbers of oxygens used to change $TeO_{4/2}$ to $O_{3/2}Te\text{–}O^-$ are much smaller in V_2O_5–TeO_2 glasses than other glass systems.

The conductivity of V_2O_5–TeO_2 glasses is attributed to electron hoping between neighbouring V^{4+} and V^{5+} [4]. Since V^{4+} ions exist in tetragonally distorted octahedral sites in V_2O_5–TeO_2 glasses [28], these are considered to be connected with $(V_2O_8)_n$ zigzag chains.

5. Conclusion

The structures of V_2O_5–TeO_2 glasses were examined by means of the ^{125}Te and ^{51}V static NMR spectroscopies. The following conclusions were obtained.

(i) The fraction of TeO_3 tp increases and that of TeO_4 tbp decreases with increasing V_2O_5 content.

(ii) The fraction of $TeO_{4/2}$ (TeO_4 tbp without a non-bridging oxygen (NBO)) decreases, while those of $O_{3/2}Te–O^-$ (TeO_4 tbp with an NBO) and $O_{1/2}Te(=O)–O^-$ (TeO_3 tp with two NBOs) increase with an increase of V_2O_5 content up to 33.3 mol%.

(iii) The fraction of VO_4 tetrahedral increases and that of VO_5 tbp decreases with increasing V_2O_5 content.

(iv) The VO_4^{3-} and $(VO_4)_n^{3n-}$ chain fractions decrease and the $(VO_3)_n^{n-}$ chain fraction increases with an increase of V_2O_5 content up to 33.3 mol%. The $(V_2O_8)_n$ zigzag chain fraction is 0% in the glasses with V_2O_5 contents less than 20 mol% and then increases with increasing V_2O_5 content. The structural units $(VO_3)_n^{n-}$, $(VO_4)_n^{3n-}$ and $(V_2O_8)_n$ chains are contained in glasses with V_2O_5 contents more than 30 mol%.

(v) Both V_2O_5 and TeO_2 can act as network formers in the V_2O_5–TeO_2 glasses. The tellurite structural units such as $TeO_{4/2}$ and $O_{3/2}Te–O^-$ mainly form a glass network in glasses with low V_2O_5 contents, while the vanadate structural units such as $(VO_3)_n^{n-}$, $(VO_4)_n^{3n-}$ and $(V_2O_8)_n$ chains mainly form a glass network in glasses with high V_2O_5 contents.

Acknowledgments

The authors thank Professor F Horii, Mrs K Omine and Dr H Kaji of Kyoto University for their helpful advice and assistance in the NMR measurements. One of the authors (TY) also acknowledges a grant from the Asahi Glass Foundation.

References

[1] Denton E P, Rawson H and Stanworth J E 1954 *Nature* **173** 1030–2
[2] Flynn B W, Owen A E and Robertson J M 1977 *Proc. 7th Int. Conf. on Amorphous and Liquid Semiconductors (Edinburgh)* pp 678–82
[3] Flynn B W and Owen A E 1981 *J. Physique Coll.* **42** C4 1005–8
[4] Dhawan V K, Mansingh A and Sayer M 1982 *J. Non-Cryst. Solids* **51** 87–103
[5] Hirashima H, Ide M and Yoshida T 1986 *J. Non-Cryst. Solids* **86** 327–35
[6] Mansingh A and Dhawan V K 1983 *Phil. Mag.* B **47** 121–38
[7] Gattef E and Dimitriev Y 1979 *Phil. Mag.* B **40** 233–42
[8] Dimitriev Y and Dimitrov V 1978 *Mater. Res. Bull.* **13** 1071–5
[9] Dimitriev Y, Dimitrov V and Arnaudov M 1983 *J. Mater. Sci.* **18** 1353–8
[10] Sakida S, Hayakawa S and Yoko T 1999 *J. Non-Cryst. Solids* **243** 13–25
[11] Sakida S, Hayakawa S and Yoko T 1999 *J. Ceram. Soc. Japan* **107** 395–402
[12] Sakida S, Hayakawa S and Yoko T *J. Am. Ceram. Soc.* submitted
[13] Hayakawa S, Yoko T and Sakka S 1994 *J. Ceram. Soc. Japan* **102** 530–6
[14] Hayakawa S, Yoko T and Sakka S 1995 *J. Non-Cryst. Solids* **183** 73–84
[15] Sakida S, Hayakawa S and Yoko T 1999 *J. Non-Cryst. Solids* **243** 1–12
[16] Collins M J, Ripmeester J A and Sawyer J F 1987 *J. Am. Chem. Soc.* **109** 4113–15
[17] Eckert H and Wachs I E 1989 *J. Phys. Chem.* **93** 6796-805
[18] Smith K A, Kirkpatrick R J, Oldfield E and Henderson D M 1983 *Am. Mineral.* **68** 1206–15
[19] Hayashi S and Hayamizu K 1990 *Bull. Chem. Soc. Japan* **63** 961–3
[20] Darriet J, Guillaume G, Wilhelmi K-A and Galy J 1972 *Acta Chem. Scand.* **26** 59–70
[21] Darriet J and Galy J 1973 *Cryst. Struct. Commun.* **2** 237–8
[22] Hayakawa S, Yoko T and Sakka S 1994 *J. Solid State Chem.* **112** 329–39
[23] Gopal R and Calvo C 1974 *Acta Crystallogr.* B **30** 2491–3
[24] Shannon R D and Calvo C 1973 *Can. J. Chem.* **51** 265–73
[25] Süsse P and Buerger M J 1970 *Z. Kristallogr.* **131** 161–74
[26] Kato K and Takayama E 1984 *Acta Crystallogr.* B **40** 102–5
[27] Philippot E 1981 *J. Solid State Chem.* **38** 26–33
[28] Chopra N and Mansingh A 1992 *J. Non-Cryst. Solids* **146** 261–6